The *Chlamydia trachomatis* IncM protein interferes with host cell cytokinesis, centrosome positioning and Golgi distribution, and contributes to the stability of the pathogen-containing vacuole

SUPPLEMENTAL MATERIAL

Maria Pequito Luís[1,2], Inês Serrano Pereira[1,2⁋], Joana N. Bugalhão[1,2⁋], Catarina N. Simões[2,3], Cristiano Mota[1,4], Maria João Romão[1,4], and Luís Jaime Mota[1,2]

[1]Associate Laboratory i4HB - Institute for Health and Bioeconomy, NOVA School of Science and Technology, NOVA University Lisbon, Caparica, Portugal.

[2]UCIBIO – Applied Molecular Biosciences Unit, Department of Life Sciences, NOVA School of Science and Technology, NOVA University Lisbon, Caparica, Portugal.

[3]Faculty of Sciences, University of Lisbon.

[4]UCIBIO – Applied Molecular Biosciences Unit, Department of Chemistry, NOVA School of Science and Technology, NOVA University Lisbon, Caparica, Portugal.

⁋These two authors equally contributed to this work.

Running title: IncM during Chlamydia infection of host cells

#Address correspondence to Luís Jaime Mota, ljmota@fct.unl.pt

Table S1. Plasmids used in this study.

Plasmid	Characteristics and construction	Source/Ref.
pVector[Pgp4^{+}] /pSVP247	Derivative of *C. trachomatis*-*E. coli* shuttle vector (p2TK2-SW2) for production of proteins with a C-terminal double hemagglutinin (2HA) tag. Contains the terminator of the *incDEFG* operon of *C. trachomatis* L2/434 (Amp^{R}).	(1)
pIncM-2HA /pFA202	Derivative of pSVP247. Enables the production of IncM-2HA under the control of the *incM* promoter (P*incM*). A DNA fragment comprising P*incM-incM* was amplified from *C. trachomatis* L2/434 chromosomal DNA using primers #1960 and #1567. The resulting DNA product was digested with KpnI and NotI and ligated into those sites of pSVP247 (Amp^{R}).	This work.
pIncM$_{1\text{-}242}$-2HA /pML22	Derivative of pSVP247. Enables the production of IncM$_{1\text{-}242}$-2HA under the control of the *incM* promoter (P*incM*). A DNA fragment comprising P*incM-incM$_{1\text{-}726}$* was amplified from pFA202 using primers #1960 and #2505. The resulting DNA product was digested with KpnI and NotI and ligated into those sites of pSVP247 (Amp^{R}).	This work.
pIncM$_{\Delta 89\text{-}288}$ /pML23	Derivative of pSVP247. Enables the production of IncM$_{\Delta 89\text{-}288}$-2HA (C-terminal of IncM with the first transmembrane domain deleted) under the control of the *incM* promoter (P*incM*). The DNA fragments comprising P*incM-incM$_{1\text{-}264}$* and *incM$_{867\text{-}1692}$* were amplified from pFA202 using primers #1960 and #2506, and #2507 and #1567. The DNA products were then fused by overlapping PCR using primers #1960 and #1567. The final DNA product was digested with KpnI and NotI and ligated into those sites of pSVP247 (Amp^{R}).	This work
pIncM$_{\Delta 34\text{-}242}$ /pML24	Derivative of pSVP247. Enables the production of IncM$_{\Delta 34\text{-}242}$-2HA (C-terminal of IncM with the second transmembrane domain) under the control of the *incM* promoter (P*incM*). The DNA fragments comprising P*incM-incM$_{1\text{-}99}$* and *incM$_{729\text{-}1692}$* were amplified from pFA202 using primers #1960 and #2508, and #2509 and #1567. The DNA products were then fused by overlapping PCR using primers #1960 and #1567. The final DNA product was digested with KpnI and NotI and ligated into those sites of pSVP247 (Amp^{R}).	This work

Table S1. Plasmids used in this study. (*Continued*).

Plasmid	Characteristics and construction	Source/Ref.
pIncM$_{C/TW3}$-2HA /pML25	Derivative of pSVP247. Enables the production of IncM$_{C/TW3}$-2HA under the control of the *incM* promoter (P*incM*) from L2/434. IncM$_{C/TW3}$ is the IncM homologue from the *C. trachomatis* C/TW3 strain. A DNA fragment comprising P*incM* was amplified from pFA202 and *incM$_{C/TW3}$* from *C. trachomatis* C/TW3 chromosomal DNA using primers #1960 and #2656, and #2655 and #1567. The DNA products were then fused by overlapping PCR using primers #1960 and #1567. The final DNA product was digested with KpnI and NotI and ligated into those sites of pSVP247 (Amp^R).	This work.
pIncM$_{E/Bour}$-2HA /pML26	Derivative of pSVP247. Enables the production of IncM$_{E/Bour}$-2HA under the control of the *incM* promoter (P*incM*) from L2/434. IncM$_{E/Bour}$ is the IncM homologue from *C. trachomatis* E/Bour strain. A DNA fragment comprising P*incM* was amplified from pFA202 and *incM$_{E/Bour}$* from *C. trachomatis* E/Bour chromosomal DNA using primers #1960 and #2656, and #2655 and #1567. The DNA products were then fused by overlapping PCR using primers #1960 and #1567. The final DNA product was digested with KpnI and NotI and ligated into those sites of pSVP247 (Amp^R).	This work.
pIncM$_{mur}$-2HA pML27	Derivative of pSVP247. Enables the production of IncM$_{mur}$-2HA under the control of the *incM* promoter (P*incM*) from L2/434. IncM$_{mur}$ is the IncM homologue from *C. muridarum* Nigg strain. A DNA fragment comprising P*incM* was amplified from pFA202 and *incM$_{mur}$* from *C. muridarum* Nigg chromosomal DNA using primers #1960 and #2658, and #2657 and #2511. The DNA products were then fused by overlapping PCR using primers #1960 and #2511. The final DNA product was digested with KpnI and NotI and ligated into those sites of pSVP247 (Amp^R).	This work.

Table S1. Plasmids used in this study. (*Continued*).

Plasmid	Characteristics and construction	Source/Ref.
pIncM$_{cav}$-2HA /pML28	Derivative of pSVP247. Enables the production of IncM$_{cav}$-2HA under the control of the *incM* promoter (P*incM*) from L2/434. IncM$_{cav}$ is the IncM homologue from *C. caviae* GPIC strain. A DNA fragment comprising P*incM* was amplified from pFA202 and *incM$_{cav}$* from *C. caviae* GPIC chromosomal DNA using primers #1960 and #2660, and #2659 and #2513. The DNA products were then fused by overlapping PCR using primers #1960 and #2513. The final DNA product was digested with KpnI and NotI and ligated into those sites of pSVP247 (Amp^R).	This work.
pET-28b(+)	Bacterial vector for production of N-terminally 6xHis-tagged proteins.	Novagen.
pJB13	Derivative of pET-28b(+). Enables production of IncM with a 6xHis tag at its N-terminus (6xHis-IncM). The DNA encoding incM was amplified from *C. trachomatis* L2/434 chromosomal DNA using primers #1872 and #1873. The resulting DNA product was digested with NdeI and EcoRI and ligated into those sites of pET-28b(+) (Km^R)	This work.

Amp^R: ampicillin resistance; Km^R: kanamycin resistance.

Table S2. DNA primers used in this study.

Number	Description	Sequence (5' → 3')
1567	CT288_NotI_Rv; reverse primer to construct pFA202, pFA203, pML23, pML24, pML25, pML26, pML29, pML30 and pCS12. Has a NotI restriction site.	GATCGCGGCCGCGGTGATTA TCTAACAGGTATTG
1803	TetR-STOP-Fwd-KpnI; forward primer to construct pFA203. Has a KpnI restriction site.	GATCGGTACCTTAAGACCCA CTTTCACATTTAA
1872	Forward primer used to construct pJB13.	CGGCAGCCATATGGTTTATTT TAGAGCTCATC
1873	Reverse primer used to construct pJB13.	GATCGAATTCTTAGTGATTAT CTAACAGG
1960	PromCT288_Fw_KpnI; forward primer to construct pFA202, pML22, pML23, pML24, pML25, pML26, pML27, pML28, pML29, pML30, pML31, and pCS12. Has a KpnI restriction site.	GATCGGTACCGCAACAATGA CAGTTTTACGC
2505	CT288-L2_242Rv_NotI; reverse primer to construct pML22. Has a NotI restriction site.	GATCGCGGCCGCTTGTATATA GTGTGCGGCTGGC
2506	CT288-L2_OL_88Rv; reverse overlap primer to construct pML23.	GTTCGAGCAAATACTTAATG CCCCGTGCAGAACAGATAAT GGTGGC
2507	CT288-L2_OL_289Fw; forward overlap primer to construct pML23.	GCCACCATTATCTGTTCTGCA CGGGGCATTAAGTATTTGCTC GAAC
2508	CT288-L2_OL_33Rv; reverse overlap primer to construct pML24.	CTAAGGATAAAGCGACTTTC AATACTTTAGCAATTTGAGG ATGCTTATCG
2509	CT288-L2_OL_243Fw; forward overlap primer to construct pML24.	CGATAAGCATCCTCAAATTG CTAAAGTATTGAAAGTCGCTT TATCCTTAG
2511	CT288-Mur_EndRv_NotI; reverse primer to construct pML27. Has a NotI restriction site.	GATCGCGGCCGCTTCGATCC AACACATACTGCG
2513	CT288-Cav_EndRv_NotI; reverse primer to construct pML28. Has a NotI restriction site.	GATCGCGGCCGCGGTAAGGG AATTGCCCTGGAGAG
2655	Pct288-ct288_OL_Fw; forward overlap primer to construct pML25 and pML26.	GTTACGGGGGAATCTCTTTCA TGGTTTATTTTAGAGCTC

Table S2. DNA primers used in this study. (*Continued*).

Number	Description	Sequence (5' → 3')
2656	Pct288-ct288_OL_Rv; reverse overlap primer to construct pML25 and pML26.	GAGCTCTAAAATAAACCATGA AAGAGATTCCCCCGTAAC
2657	Pct288-288(Mur)_OL_F; forward overlap primer to construct pML27.	GTTACGGGGGAATCTCTTTCAT GGTTTATTTTAAAGCTG
2658	Pct288-288(Mur)_OL_R; reverse overlap primer to construct pML27.	CAGCTTTAAAATAAACCATGA AAGAGATTCCCCCGTAAC
2659	Pct288-288(Cav)_OL_F; forward overlap primer to construct pML28.	GTTACGGGGGAATCTCTTTCAT GTCTGAGCCTAAGCC
2660	Pct288-288(Cav)_OL_R; reverse overlap primer to construct pML28.	GGCTTAGGCTCAGACATGAAA GAGATTCCCCCGTAAC

Table S3. *C. trachomatis* strains used and constructed in this study.

Strains	Description	Source/Refs.
L2/434/Bu ACE051	Wild-type strain (originally from Tony Maurelli's lab; University of Florida).	From Derek J. Fisher
incM::aadA	Derivative of L2/434/Bu ACE051 where *incM* is inactivated by a group II intron carrying spectinomycin resistance gene.	(2)
incM::aadA (pIncM-2HA)	Derivative of *incM::aadA* carrying a plasmid encoding IncM-2HA under the control of the *incM* promoter (from the L2/434 strain).	This work.
incM::aadA (pIncM$_{C/TW3}$-2HA)	Derivative of *incM::aadA* carrying a plasmid encoding the IncM homologue from the *C. trachomatis* C/TW3 strain (IncM $_{C/TW3}$-2HA) under the control of the *incM* promoter (from the L2/434 strain).	This work.
incM::aadA (pIncM$_{E/Bour}$-2HA)	Derivative of *incM::aadA* carrying a plasmid encoding the IncM homologue from the *C. trachomatis* E/Bour strain (IncM$_{E/Bour}$-2HA) under the control of the *incM* promoter (from the L2/434 strain).	This work.
incM::aadA (pIncM$_{mur}$-2HA)	Derivative of *incM::aadA* carrying a plasmid encoding the IncM homologue from *C. muridarum* (IncM$_{mur}$-2HA) under the control of the *incM* promoter (from the L2/434 strain).	This work.
incM::aadA (pIncM$_{cav}$-2HA)	Derivative of *incM::aadA* carrying a plasmid encoding the IncM homologue from *C. caviae* (IncMcav-2HA) under the control of the *incM* promoter (from the L2/434 strain).	This work.
incM::aadA (pIncM$_{1-242}$-2HA)	Derivative of *incM::aadA* carrying a plasmid encoding IncM$_{1-242}$-2HA under the control of the *incM* promoter (from the L2/434 strain).	This work.
incM::aadA (pIncM$_{\Delta 89-288}$-2HA)	Derivative of *incM::aadA* carrying a plasmid encoding IncM$_{\Delta 89-288}$ under the control of the *incM* promoter (from the L2/434 strain).	This work.
incM::aadA (pIncM$_{\Delta 34-242}$-2HA)	Derivative of *incM::aadA* carrying a plasmid encoding IncM$_{\Delta 34-242}$ under the control of the *incM* promoter (from the L2/434 strain).	This work.

Figure S1

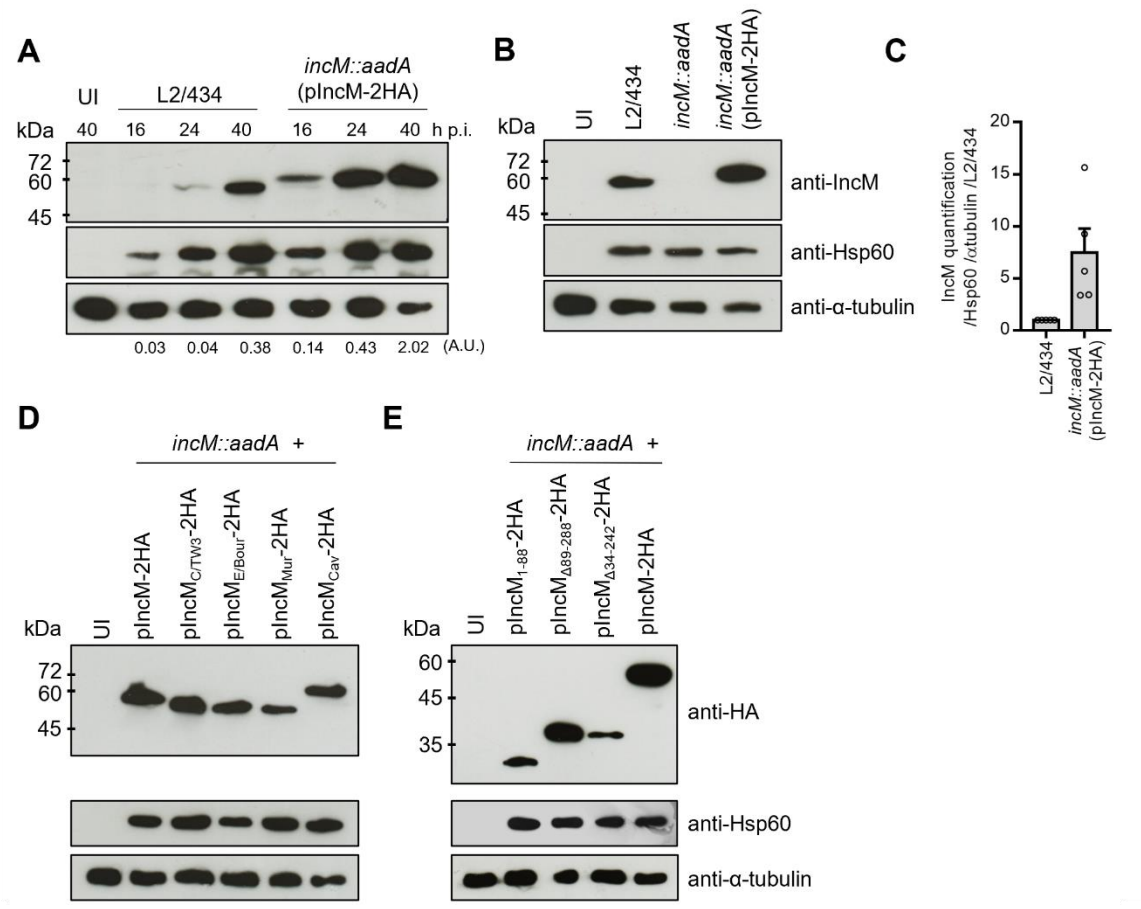

Figure S1. Assessment and quantification of IncM production by immunoblotting. HeLa cells were left uninfected (UI) or were infected at a multiplicity of infection of 1.5 with the indicated strains: *C. trachomatis* L2/434, *incM::aadA*, or *incM*::*aadA* derived-strains harboring the indicated plasmids encoding IncM from the *C. trachomatis* L2/434 strain or orthologues from C/TW3, E/Bour, *C. muridarum* Nigg, and *C. caviae* GPIC, all with a C-terminal 2HA epitope tag. At the indicated times post-infection (p.i.) (A), at 40 h p.i. (B), or at 30 h p.i. (C), whole cell lysates were collected and analyzed by immunoblotting with antibodies against IncM or HA. Antibodies against *C. trachomatis* Hsp60 and α-tubulin were also used to control the loading of bacteria and host cells, respectively. In (**A**) and in **(B)** (and in four other similar replicates), the band corresponding to IncM in each lane of the anti-IncM blots was quantified by densitometry relative to the corresponding bands of Hsp60 and tubulin using Fiji software (3). In (A) the calculated IncM/Hsp60/tubulin values are indicated as arbitrary units (A.U,). In (C), the values obtained from the quantification of blots as (B) were normalized to L2/434 (mean ± standard error of the mean from 5 independent experiments).

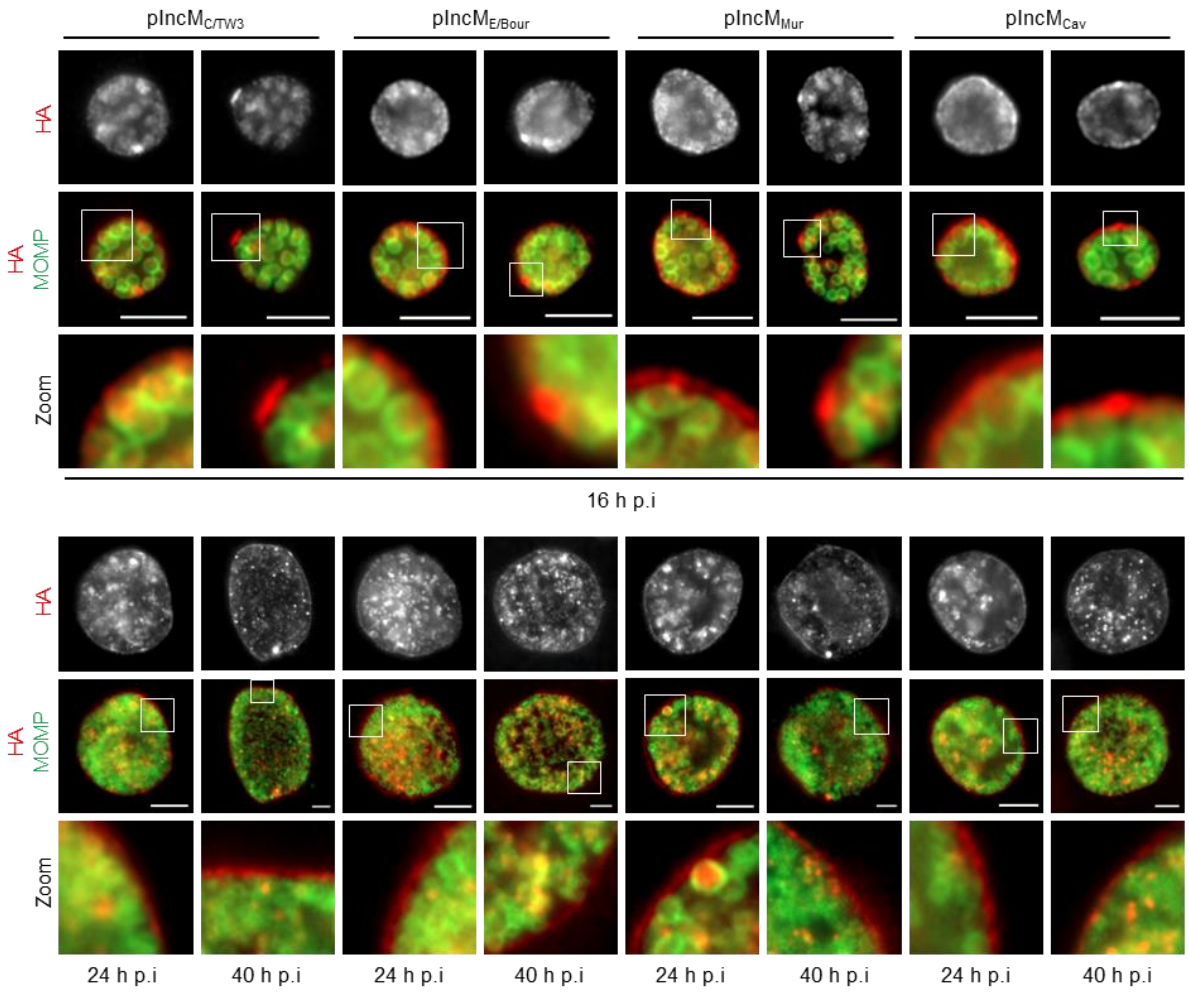

Figure S2. Localization of IncM orthologues during infection. HeLa cells were infected at a multiplicity of infection of 0.3 with *C. trachomatis incM*::*aadA* derived-strains harboring the indicated plasmids encoding IncM from *C. trachomatis* L2/434 strain or orthologues from C/TW3, E/Bour, *C. muridarum* Nigg, and *C. caviae* GPIC, all with a C-terminal 2HA epitope tag. Cells were fixed with methanol and immunolabeled with anti-*C. trachomatis* Major Outer Membrane Protein (MOMP; green) and anti-HA (red) antibodies. The localization of IncM-2HA was assessed by fluorescence microscopy at the indicated times post-infection (p.i). Scale bars, 5 µm.

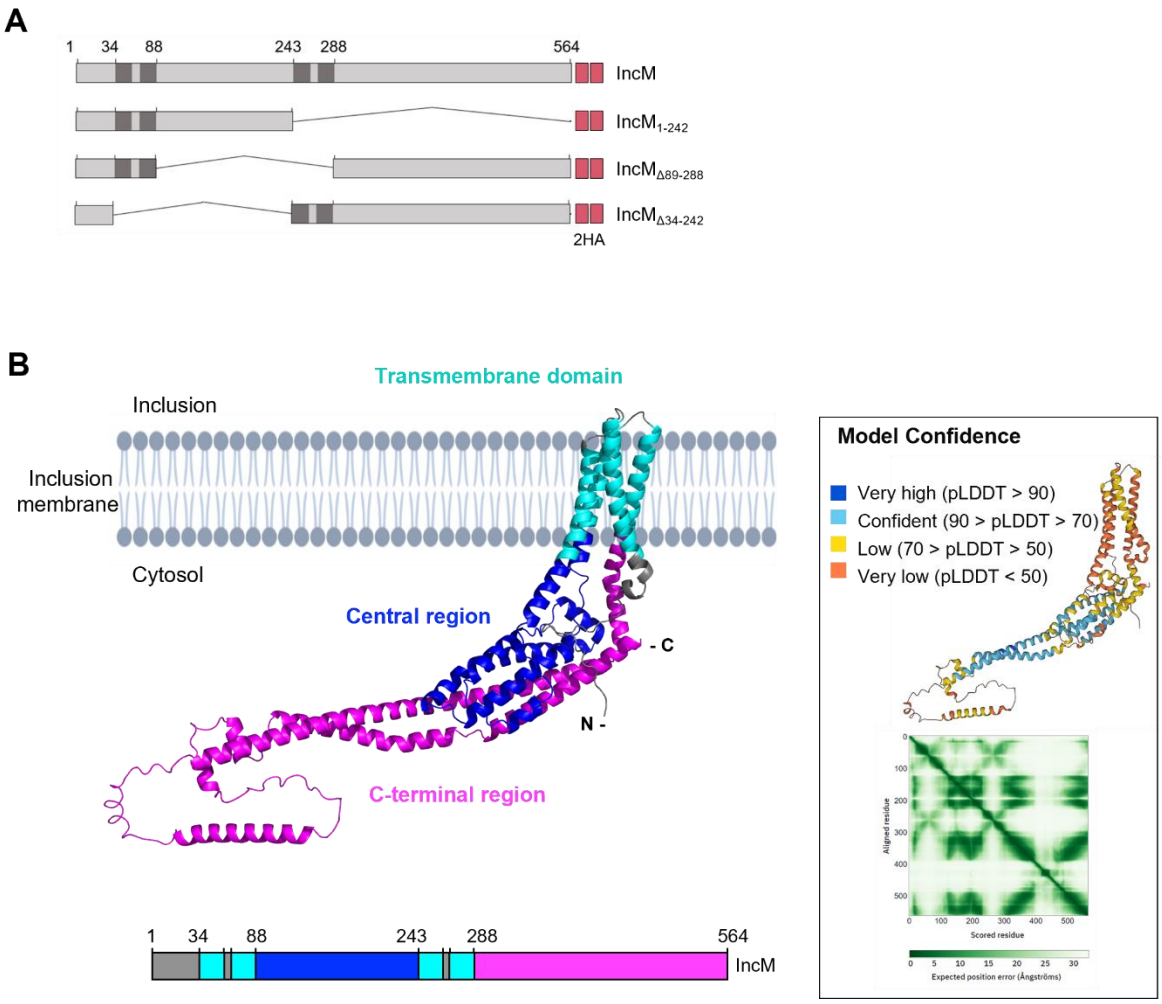

Figure S3. Representation of truncated IncM proteins studied and of IncM regions in a structural model predicted by Alphafold2. (A) Schematic representation of IncM (564 amino acid residues) and truncated IncM proteins studied, carrying a C-terminal 2HA tag. The numbers indicate amino acid residues, and the darker bars indicate predicted hydrophobic regions. (B) IncM structural model calculated by Alphafold2 (4) with its regions highlighted in colors and linear schematic representation. Transmembrane domains are represented in cyan, the central region in blue and the C-terminal region in magenta. The inset on the right depict the confidence of the model obtained with Alphafold2.

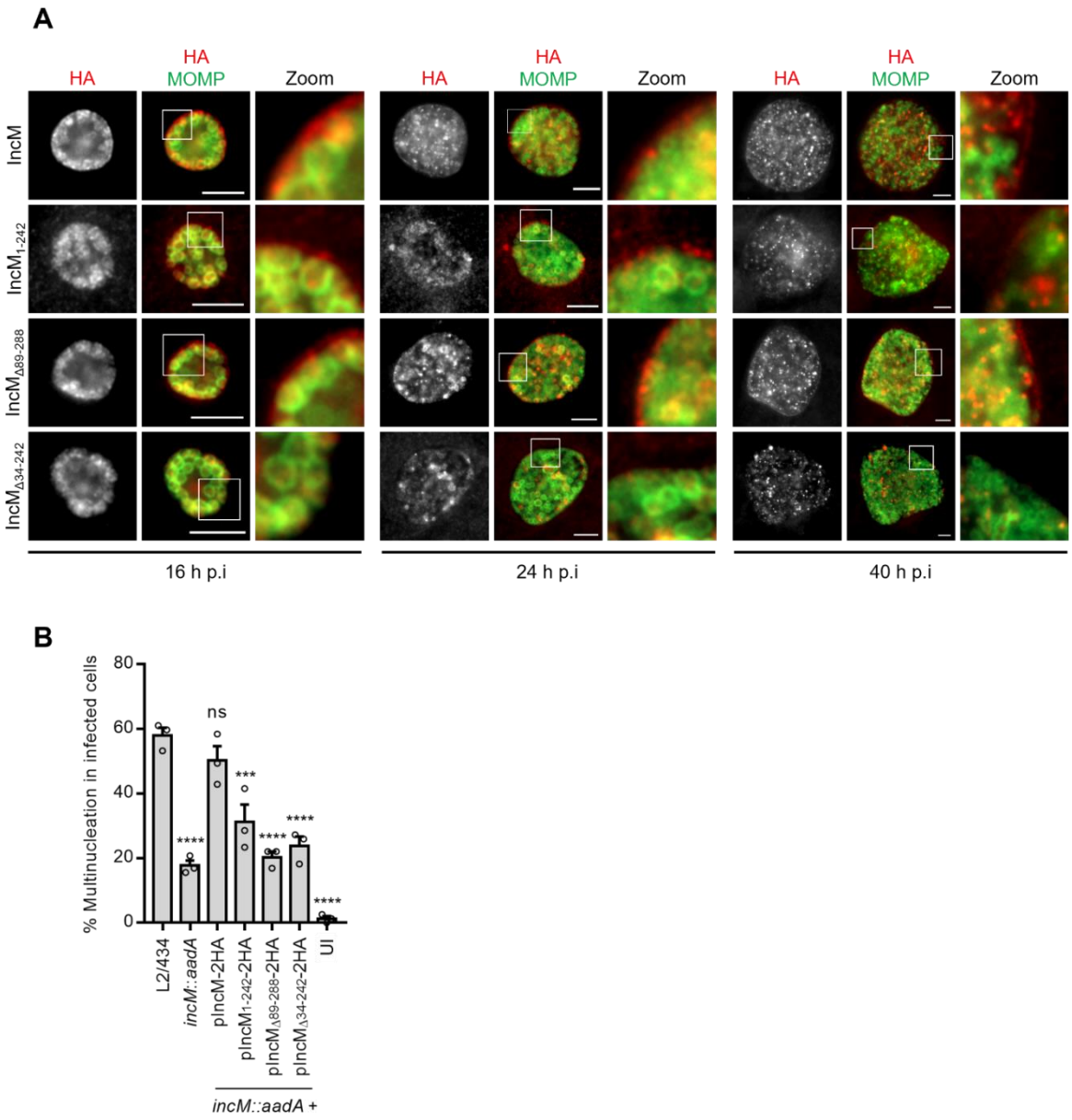

Figure S4. The ability of IncM to induce multinucleation in infected cells appears to require its host cytosol-exposed larger regions. HeLa cells were left uninfected or were infected at a multiplicity of infection (MOI) of 0.1 with *C. trachomatis* strains L2/434, *incM::aadA* or *incM::aadA* harboring plasmids encoding 2HA-tagged IncM proteins depicted in (Fig. S3A) and as indicated. In (A), cells were fixed at the indicated times post-infection (p.i.) with methanol, immunolabeled with anti-*C. trachomatis* Major Outer Membrane Protein (MOMP; green) and anti-HA (red) antibodies and imaged by fluorescence microscopy; scale bars, 5 µm. In (B) at 40 h p.i., cells were fixed with methanol, immunolabeled with anti-MOMP antibodies, stained for the nuclei with 4′,6-diamidino-2-phenylindole (DAPI), and analyzed by fluorescence microcopy. Uninfected (UI) and infected cells with more than one nucleus were enumerated. Values represent mean ± standard error of the mean, n=3, ≥ 70 cells per experiment; P-values were obtained using one-way ANOVA and Dunnet's post-hoc test analysis relative to cells infected by the L2/434 strain; ns, not significant; **, P < 0.01; ***, P < 0.001; ****, P < 0.0001.

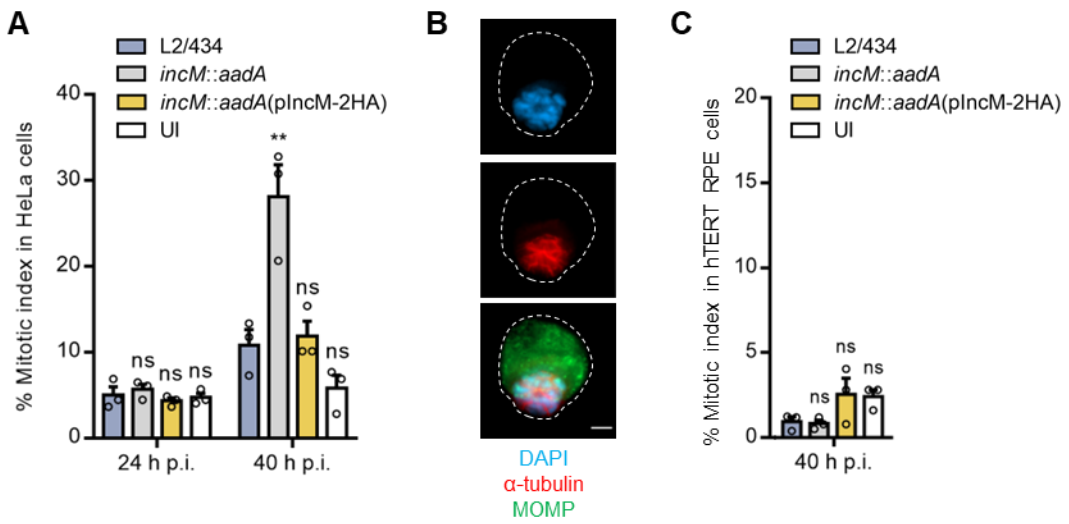

Figure S5. Differences in mitotic index in infected cells do not explain the ability of IncM to induce multinucleation in infected cells. HeLa (A and B) or hTERT-RPE1 (C) cells were left uninfected or were infected at a multiplicity of infection of 0.1 with *C. trachomatis* strains L2/434, *incM::aadA*, or *incM::aadA* harboring a plasmid encoding IncM with a C-terminal 2HA epitope tag (pIncM-2HA). Cells were fixed at 24 and 40 h post-infection (p.i.), immunolabelled with anti-*C. trachomatis* Major Outer Membrane Protein (MOMP) (green) and anti-α-tubulin (microtubules, red) antibodies, stained for the nuclei with 4′,6-diamidino-2-phenylindole (DAPI; blue), and analyzed by fluorescence microscopy. (**A** and **C**) The number of infected cells in mitosis was enumerated. (B) Representative *incM::aadA*-infected HeLa cells at 40 h p.i. with abnormal mitotic spindles; scale bars, 5 µm. Values in (A) and (C) represent mean ± standard error of the mean, n=3, 250 cells per experiment; P-values were obtained using one-way ANOVA and Dunnet's post-hoc test analysis relative to cells infected by the L2/434 strain; ns, not significant; **, $P < 0.01$.

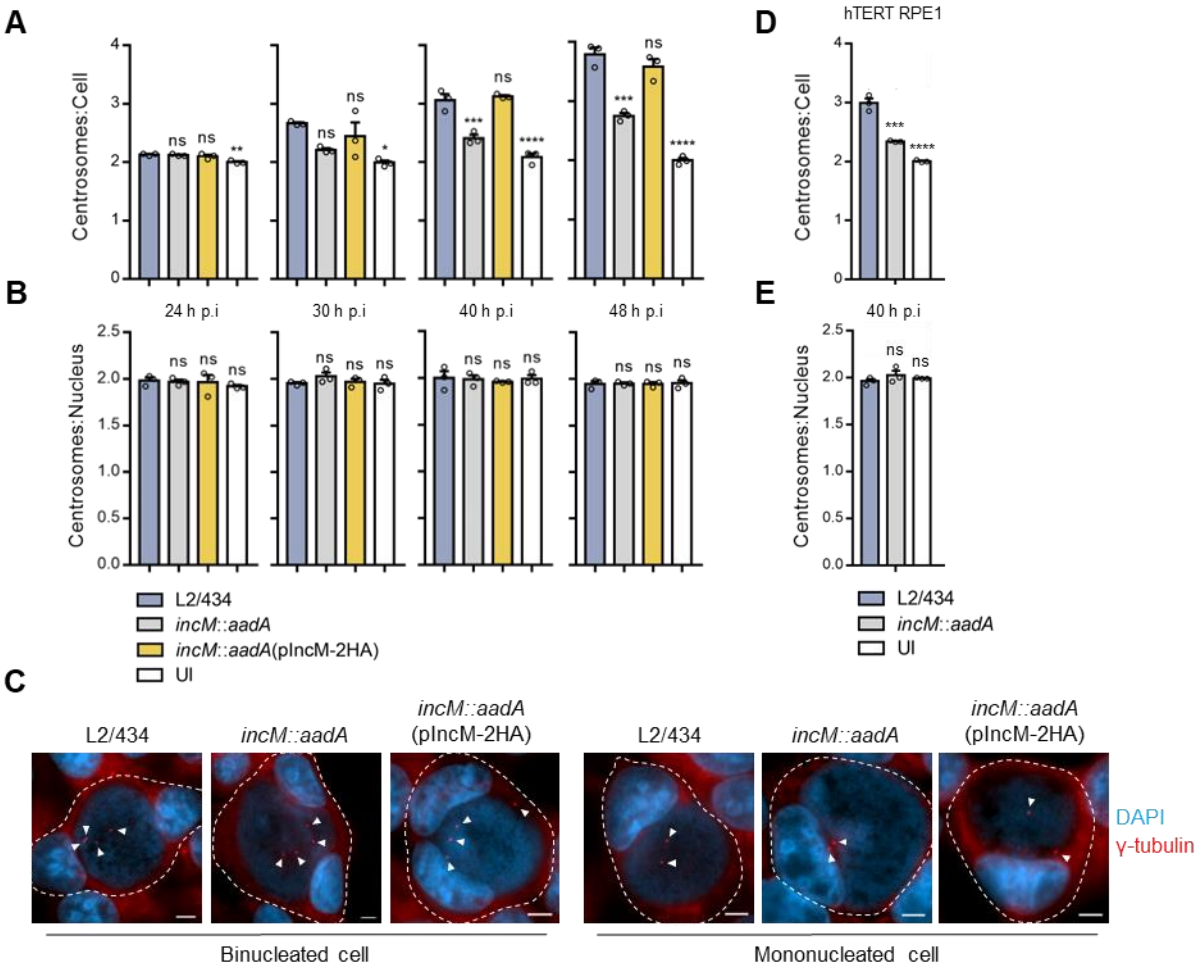

Figure S6. IncM does not promote centrosome amplification in infected cells. HeLa (A, B and C) and hTERT-RPE1 (D and E) cells were left uninfected or were infected at a multiplicity of infection of 0.1 with *C. trachomatis* strains L2/434, *incM::aadA*, or *incM::aadA* harboring a plasmid encoding IncM with a C-terminal 2HA epitope tag (pIncM-2HA). Cells were fixed with methanol at the indicated times post-infection (p.i.), immunolabelled for the centrosome with γ-tubulin antibodies (red), stained for the nuclei and the chlamydiae with 4′,6-diamidino-2-phenylindole (DAPI; blue), and analyzed by fluorescence microscopy. The number of centrosomes per cell (A and D) and per nucleus (B and E) was enumerated. (**C**) Representative binucleated (left panel) or mononucleated (right panel) HeLa cells at 40 h p.i. are shown; arrowheads point to the centrosomes; scale bars, 5 μm. Values in (A), (B), (D), and (E) represent mean ± SEM, n=3, ≥ 30 cells per experiment; P-values were obtained using one-way ANOVA and Dunnet's post-hoc test analysis relative to cells infected by the L2/434 strain; ns, not significant; *, $P < 0.05$; **, $P < 0.01$; ***, $P < 0.001$; ****, $P < 0.0001$.

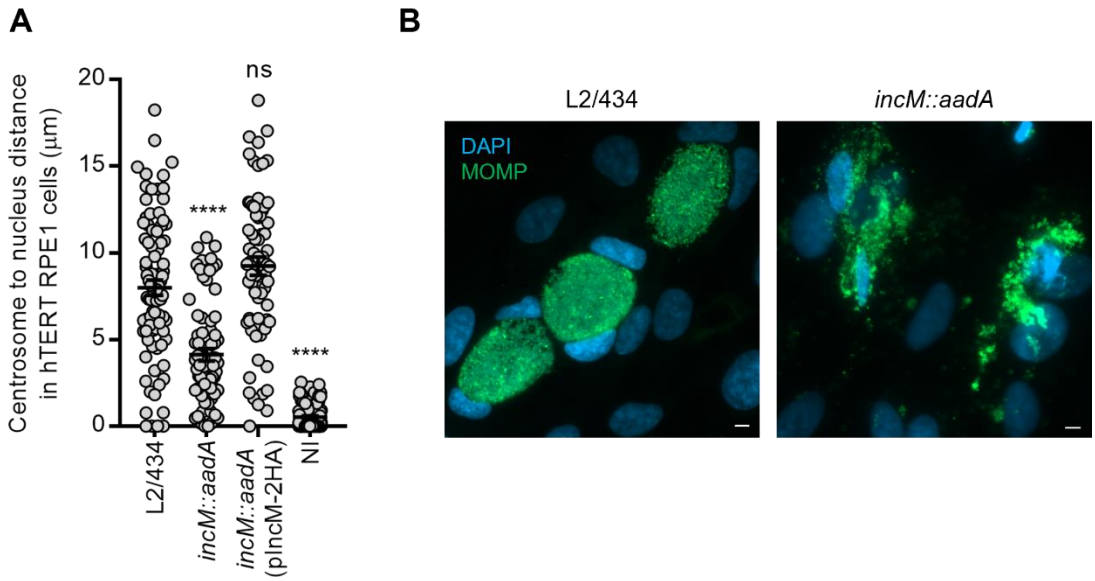

Figure S7. IncM contributes to host cell centrosome positioning and to inclusion stability in hTERT RPE1 cells. hTERT RPE1 cells were left uninfected or infected at a multiplicity of infection of 0.1 for 40 h with *C. trachomatis* strains L2/434, *incM::aadA* (A and B)or *incM::aadA* harboring a plasmid encoding IncM with a C-terminal 2HA epitope tag (pIncM-2HA; in A). (**A**) Cells were fixed with methanol and immunolabelled with anti-*C. trachomatis* Major Outer Membrane Protein (MOMP) and γ-tubulin (centrosome) antibodies, stained with 4′,6-diamidino-2-phenylindole (DAPI) (nuclei), and analyzed by fluorescence microscopy. The distance of the centrosomes to the closest point in the nucleus was measured using Fiji (3). Values represent mean ± standard error of the mean, n=3, ≥ 30 cells per experiment; P-values were obtained using one-way ANOVA and Dunnet's post-hoc test analysis relative to cells infected by the L2/434 strain. (**B**) Cells were fixed with methanol, labelled with anti-MOMP (green), stained with DAPI (nuclei; blue), and analyzed by fluorescence microscopy. Illustrative images are shown; scale bars, 5 µm**.**

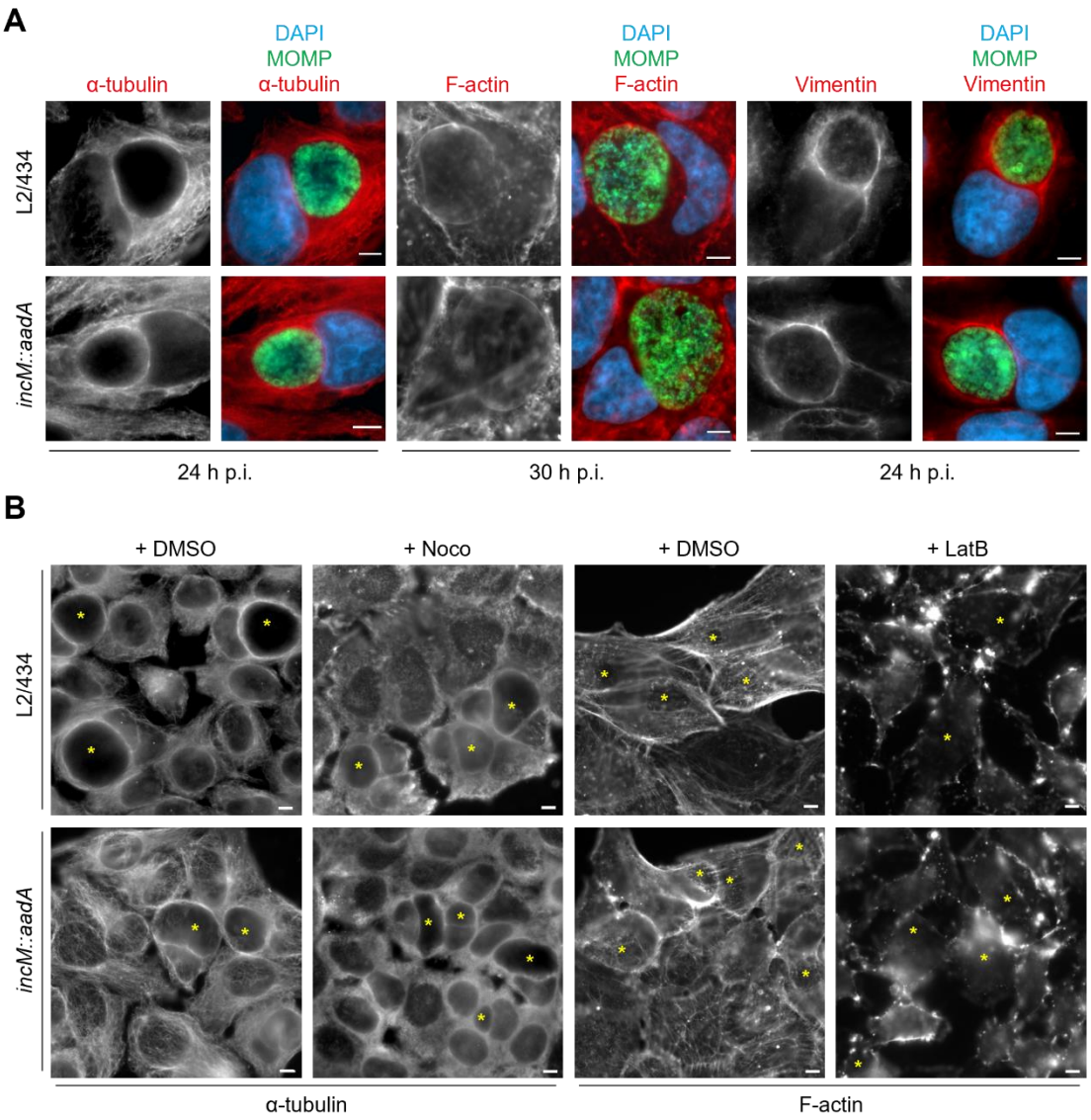

Figure S8. Cytoskeleton cages around the inclusion and control of nocodazole and latrunculin B activity on microtubules and actin filaments, respectively. HeLa cells were infected at a multiplicity of infection 0.1 for the indicated times post-infection (p.i.; in A, or for 30 h p.i. (in B) with *C. trachomatis* strains L2/434 or *incM::aadA*. (**A**) Cells were fixed with methanol (for labelling of microtubules and intermediate filaments) or paraformaldehyde 4% (w/v) (for labelling of filamentous actin; F-actin), labelled with anti-*C. trachomatis* Major Outer Membrane Protein (MOMP) (green) and anti-α-tubulin (microtubules; red) or anti-vimentin (intermediate filaments, red) antibodies, or fluorophore-conjugated phalloidin (F-actin; red), and stained with 4′,6-diamidino-2-phenylindole (DAPI) (nuclei; blue), and analyzed by fluorescence microscopy. (**B**) At 30 h p.i., after being treated with nocodazole (Noco) or latrunculin B (LatB), as described in Materials and Methods, or with solvent dimethyl sulfoxide (DMSO) as control, cells were fixed with methanol (labelling of microtubules) or paraformaldehyde 4% (w/v) (labelling of filamentous actin; F-actin), and labelled with anti-α-tubulin (microtubules) antibodies or fluorophore-conjugated phalloidin (F-actin). Cells were analyzed by fluorescence microscopy to verify cytoskeleton depolymerization after drug treatment. * Marks the chlamydial inclusions. Scale bars, 5 μm.

Supplemental References

1. da Cunha M, Pais SV, Bugalhao JN, Mota LJ. 2017. The *Chlamydia trachomatis* type III secretion substrates CT142, CT143, and CT144 are secreted into the lumen of the inclusion. PLoS One 12:e0178856. https://doi:10.1371/journal.pone.0178856.
2. Almeida F, Luis MP, Pereira IS, Pais SV, Mota LJ. 2018. The Human Centrosomal Protein CCDC146 Binds *Chlamydia trachomatis* Inclusion Membrane Protein CT288 and Is Recruited to the Periphery of the *Chlamydia*-Containing Vacuole. Front Cell Infect Microbiol 8:254. https://doi:10.3389/fcimb.2018.00254.
3. Schindelin J, Arganda-Carreras I, Frise E, Kaynig V, Longair M, Pietzsch T, Preibisch S, Rueden C, Saalfeld S, Schmid B, Tinevez JY, White DJ, Hartenstein V, Eliceiri K, Tomancak P, Cardona A. 2012. Fiji: an open-source platform for biological-image analysis. Nat Methods 9:676-82. https://doi:10.1038/nmeth.2019.
4. Jumper J, Evans R, Pritzel A, Green T, Figurnov M, Ronneberger O, Tunyasuvunakool K, Bates R, Zidek A, Potapenko A, Bridgland A, Meyer C, Kohl SAA, Ballard AJ, Cowie A, Romera-Paredes B, Nikolov S, Jain R, Adler J, Back T, Petersen S, Reiman D, Clancy E, Zielinski M, Steinegger M, Pacholska M, Berghammer T, Bodenstein S, Silver D, Vinyals O, Senior AW, Kavukcuoglu K, Kohli P, Hassabis D. 2021. Highly accurate protein structure prediction with AlphaFold. Nature 596:583-589. https://doi:10.1038/s41586-021-03819-2.